of CF_2 to act as a strong acceptor is essential for the integrity of the iron-iridium compound **1a**.

Conclusions

An iridium(I) complex, $IrCl(CO)(PMe_2Ph)_2$, has been shown to undergo oxidative addition by a cationic difluorocarbene complex, $[CpFe(CO)_2(CF_2)]^+$. The product is an unusual CF_2-bridged compound with an Fe-Ir bond. The iron difluorocarbene cation can be displaced by using BCl_3, which generates the BCl_3 adduct of $Ir(Cl)(CO)(PMe_2Ph)_2$.

Acknowledgment. This research was supported by the NSF through the Synthetic Inorganic and Organometallic Chemistry Program (Grant CHE-8506011).

Registry No. **1a**, 112173-03-2; **1a**·CH_2Cl_2, 112318-74-8; **1b**, 112318-73-7; $[CpFe(CO)_2(CF_2)][BF_4]$, 88211-34-1; $Ir(Cl)(CO)(PMe_2Ph)_2$, 21209-82-5; $[CpFe(CO)_2(CF_2)][BPh_4]$, 112173-04-3; $[CpFe(CO)_3][BPh_4]$, 31781-41-6; $Mn(CO)_5CCl_3$, 86392-59-8; $Mn(CO)_5CBr_3$, 86392-60-1; $CpFe(CO)_2CCl_3$, 86392-66-7; $K[BPh_4]$, 3244-41-5; BCl_3, 10294-34-5; Fe, 7439-89-6; Ir, 7439-88-5; BCl_3·$Ir(Cl)(CO)(PMe_2Ph)_2$, 112481-46-6.

Supplementary Material Available: Tables of anisotropic thermal parameters for non-hydrogen atoms and additional bond lengths and angles, a ^{19}F NMR spectrum of CF_2 resonances of **1a**, and a ^{31}P NMR spectrum of **1a** (4 pages); a table of observed and calculated structure factors (34 pages). Ordering information is given on any current masthead page.

Contribution from the Department of Chemistry, Northwestern University, Evanston, Illinois 60201, and Corporate Research Laboratory, Exxon Research and Engineering Company, Annandale, New Jersey 08801

Protonation and Bonding in Heterometallic Butterfly Carbide Clusters

Joseph A. Hriljac,† Suzanne Harris,*‡ and Duward F. Shriver*†

Received June 5, 1987

The protonation of the heterometallic butterfly carbide clusters $[CrFe_3(CO)_{13}C]^{2-}$, $[WFe_3(CO)_{13}C]^{2-}$, $[MnFe_3(CO)_{13}C]^-$, and $[RhFe_3(CO)_{12}C]^-$ was studied by multinuclear NMR spectroscopy, and the protonation products were characterized. With 1 equiv of acid all of the clusters protonate at the carbide ligand to produce an agostic C-H-Fe linkage with a wingtip iron atom. This contrasts with the behavior of the isoelectronic homometallic cluster $[Fe_4(CO)_{12}C]^{2-}$, for which the first proton adds across the Fe-Fe hinge of the cluster. Fenske-Hall molecular orbital calculations were carried out for $[RhFe_3(CO)_{12}C]^-$ and $[MnFe_3(CO)_{13}C]^-$, and the electronic structures of these heterometallic clusters were compared with that of $[Fe_4(CO)_{12}C]^{2-}$. The introduction of a heterometal perturbs the metal framework bonding orbitals, and the relative energies of the resulting orbitals depend on the nature of the heterometal. In both heterometallic clusters the nature of the HOMO correlates with the site of proton attack.

Introduction

Reactivity of a cluster-bound carbide ligand was first reported by Bradley and co-workers, who discovered that the oxidative degradation of a hexametallic iron carbide cluster leads to a tetranuclear cluster with a functionalized carbide ligand:[1]

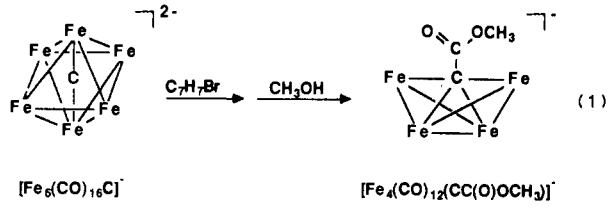

This work was quickly followed by the isolation and characterization of a family of four-iron carbide clusters: $[Fe_4(CO)_{12}C]^{2-}$, $[HFe_4(CO)_{12}C]^-$, and $Fe_4(CO)_{13}C$.[2-4] All of these compounds display reactivity at the carbide ligand, and several reactions involving C-H or C-C bond formation have been reported (Scheme I).[1-6]

Earlier we reported the syntheses of the mixed-metal butterfly carbide clusters $[CrFe_3(CO)_{13}C]^{2-}$, $[WFe_3(CO)_{13}C]^{2-}$, $[MnFe_3(CO)_{13}C]^-$, and $[RhFe_3(CO)_{12}C]^-$.[7,8] These clusters are all "isoelectronic" with the four-iron carbide cluster $[Fe_4(CO)_{12}C]^{2-}$, but they are characterized by the presence of a heterometal occupying one of the hinge positions in the metal butterfly framework. In this paper we describe a study aimed at determining how both the reactivity and the electronic structure of these clusters are affected by the introduction of a heterometal into the metal butterfly framework. It is quite common for bimetallic catalysts to exhibit activity that is greater than the sum of the activities of the individual metals;[9] so it is of interest to explore how the presence of a heterometal in a molecular cluster affects the reactivity. It is equally important, however, to study how the introduction of a heterometal alters the electronic structure of a

Scheme I

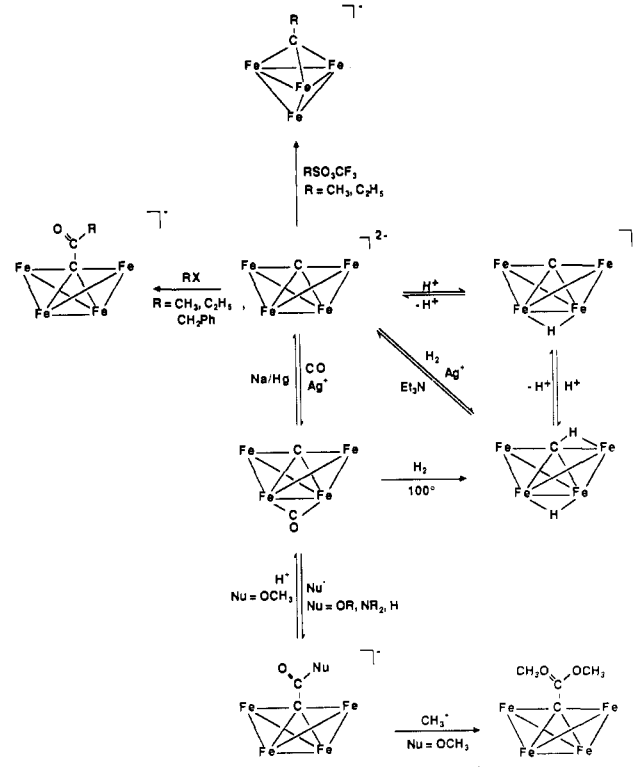

† Northwestern University.
‡ Exxon Research and Engineering Co.

(1) (a) Bradley, J. S.; Ansell, G. B.; Hill, E. W. *J. Am. Chem. Soc.* **1979**, *101*, 7417. (b) Bradley, J. S.; Hill, E. W.; Ansell, G. B.; Modrick, M. A. *Organometallics* **1982**, *1*, 1634.

0020-1669/88/1327-0816$01.50/0

Table I. IR Data in the C–O Stretching Region for Selected Heterometallic Carbide Cluster Derivatives

compd	medium	ν_{CO},[a] cm^{-1}
$[PPN][CrFe_3(CO)_{13}(CH)]$	CH_2Cl_2	2063 vw, 2006 s, 1985 s, 1970 sh, 1937 sh, 1885 vw, br, 1831 w, br
$[PPN][CrFe_3(CO)_{13}(CH)]$	Nujol	2063 vw, 1998 vs, 1983 s, 1962 s, 1936 sh, 1929 s, 1885 sh, 1875 m, 1837 m
$[PPN][WFe_3(CO)_{13}(CH)]$	CH_2Cl_2	2020 sh, 2006 s, 1997 sh, 1972 sh, 1931 w, sh
$[PPN][WFe_3(CO)_{13}(CH)]$	Nujol	2000 s, 1990 sh, 1977 s, 1959 s, 1929 s, 1886 m, 1853 m
$HCrFe_3(CO)_{13}(CH)$	pentane	2057 sh, 2042 s, 2033 s, 2024 sh, 2011 sh, 1988 w, 1962 w, 1893 w
$HCrFe_3(CO)_{13}(CH)$	Nujol	2102 w, 2060 sh, 2047 s, 2024 s, 2003 sh, 1990 sh, 1970 m, 1940 m, 1845 m
$HWFe_3(CO)_{13}(CH)$	pentane	2055 s, 2044 s, 2033 s, 2023 sh, 2011 sh, 1983 w, 1965 w, 1920 w
$HWFe_3(CO)_{13}(CH)$	Nujol	2102 w, 2060 s, 2024 sh, 2011 s, 1983 sh, 1966 s, 1940 s, 1870 s

[a] vs = very strong; s = strong; m = medium; w = weak; vw = very weak; br = broad; sh = shoulder.

cluster. Although numerous heterometallic clusters have been prepared in recent years, there is no systematic understanding of how either the reactivity or electronic structure of a cluster is influenced by the introduction of a heterometal. The butterfly carbides offer an opportunity to systematically study changes in both reactivity and electronic structure in a group of related homometallic and heterometallic clusters and to then compare and relate these changes. Insights gained from a study such as this can begin to provide us with a better understanding of the differences between homometallic and heterometallic clusters.

The reaction that was chosen for this study is protonation. The heterometallic cluster $[Fe_4(CO)_{12}C]^{2-}$, in combination with 1 equiv of strong acid, results in the formation of $[HFe_4(CO)_{12}C]^-$, for which the proton has added across the two iron atoms on the hinge. A second mole of acid yields $HFe_4(CO)_{12}(CH)$.[2,3] This novel methylidyne cluster (Scheme I) exhibits an interesting agostic[10] interaction between the methylidyne proton and one of the wingtip metal atoms.[2,11] Theoretical electronic structure studies have shown that the reactivity of $[Fe_4(CO)_{12}C]^{2-}$ is consistent with the orbital structure of the cluster.[12,13] In this paper we describe the reactivity of the heterometallic carbide clusters toward protonation and the characterization of these products. We also present the results of molecular orbital calculations for $[RhFe_3(CO)_{12}C]^-$ and $[MnFe_3(CO)_{13}C]^-$ and show how the presence of the heterometal in the butterfly framework causes changes in the orbital structure. These changes are found to be consistent with the observed reactivity.

Table II. ^1H NMR Data for Selected Carbide Cluster Derivatives[a]

compd	conditions	^1H NMR data, ppm
$[PPN][CrFe_3(CO)_{13}(CH)]$	CD_2Cl_2, +20 °C	0.52
$HCrFe_3(CO)_{13}(CH)$	CD_2Cl_2, +20 °C	−0.17, −18.41
$[PPN][WFe_3(CO)_{13}(CH)]$	CD_2Cl_2, +20 °C	1.58, −15.33
$HWFe_3(CO)_{13}(CH)$	CD_2Cl_2, +20 °C	0.02 (J_{HW} = 9.1 Hz), −15.88 (J_{HW} = 30.3 Hz)
$MnFe_3(CO)_{13}(CH)$[b]	CD_2Cl_2, +20 °C	−0.33
$RhFe_3(CO)_{12}(CH)$[b]	CD_2Cl_2, −90 °C	−1.48
$HFe_4(CO)_{12}(CH)$[c]	d	−1.31 (J_{HH} = 0.9 Hz), −27.95 (J_{HH} = 0.9 Hz)

[a] All shifts in ppm downfield of TMS; cation resonances not reported. [b] Reference 8. [c] References 2 and 11. [d] Not reported.

Experimental Section

General Procedures. All manipulations were performed under an atmosphere of purified nitrogen employing standard Schlenk techniques or in a Vacuum/Atmospheres drybox equipped with a recirculator and Dri-Train system.[14] Solvents were distilled from appropriate drying agents (CH_2Cl_2, from P_2O_5; Et_2O and methylcyclohexane, from Na/Ph_2CO; 2-PrOH, from Mg/I_2; C_5H_{12}, from 4A molecular sieves) before use. Fluorosulfuric acid, trifluoromethanesulfonic acid, and methyl trifluoromethanesulfonate were distilled under vacuum before use. The heterometallic carbide clusters and $MnFe_3(CO)_{13}(CH)$ were synthesized by literature methods.[7,8]

IR spectra (Table I) were recorded with a Perkin-Elmer 283 spectrophotometer using 0.1-mm CaF_2 solution cells or as Nujol mulls between KBr plates. IR spectra were calibrated with the 1601-cm^{-1} band of polystyrene. NMR spectra (Tables II and III) were recorded with either a JEOL FX-270 (^1H, 269.65 MHz; ^{13}C, 67.8 MHz) or Varian XL-400 (^1H, 399.942 MHz; ^{13}C, 100.577 MHz) spectrometer. All shifts are reported downfield from TMS and were referenced to the solvent resonance (^1H, $CHDCl_2$, 5.32 ppm; ^{13}C, CD_2Cl_2, 53.8 ppm). In addition to the determination of NMR spectra for fully characterized compounds, NMR data were collected on the products of low-temperature protonation (−80 °C) of $[CrFe_3(CO)_{13}C]^-$ and $[WFe_3(CO)_{13}C]^-$. In neither case was evidence obtained for an initial metastable protonation product. Mass spectra were recorded by Dr. D. L. Hung of the Northwestern University Analytical Services Laboratory with a Hewlett-Packard HP5905A spectrometer using 70-eV ionization and analyzed with MASPAN.[15] Elemental analyses were performed by Galbraith Laboratories.

Synthesis of $[PPN][CrFe_3(CO)_{13}(CH)]$. A flask was charged with 0.500 g (0.299 mmol) of $[PPN]_2[CrFe_3(CO)_{13}C]$ and a magnetic stirbar. The flask was immersed in a −78 °C cold bath, and 5 mL of CH_2Cl_2 was slowly introduced via syringe. With stirring, 26 μL (0.29 mmol) of HSO_3CF_3 was added. After 10 min, the cold bath was removed and the solution slowly warmed. After the solution reached room temperature, it was evaporated to dryness. The residue was extracted with a 10-mL portion of Et_2O. The brown solution was filtered, and then 10 mL of 2-PrOH and 40 mL of pentane were introduced to produce black crystals. Yield: 0.252 g, 74%. Anal. Calcd (found) for $C_{50}H_{31}NCrFe_3O_{13}P_2$: C, 52.90 (52.70); H, 2.75 (3.19); N, 1.23 (1.28); Cr, 4.58 (3.98); Fe, 14.76 (14.64).

Synthesis of $[PPN][WFe_3(CO)_{13}(CH)]$. This compound was prepared in a fashion analogous to that for the Cr analogue. Yield: 0.285 g, 81%. Anal. Calcd (found) for $C_{50}H_{31}NFe_3WO_{13}P_2$: C, 47.39 (46.60); H, 2.47 (2.54); N, 1.10 (1.01); Fe, 13.22 (12.63); W, 14.51 (12.47).

Synthesis of $HCrFe_3(CO)_{13}(CH)$. A flask was charged with 0.500-g (0.299-mmol) sample of $[PPN]_2[CrFe_3(CO)_{13}C]$ and immersed in a −78 °C cold bath. A 10-μL portion of CH_2Cl_2 was slowly introduced via syringe, and with stirring, 35 μL (0.61 mmol) of HSO_3F, or an equimolar amount of HSO_3CF_3, was added. After 10 min the cold bath was re-

(2) (a) Tachikawa, M.; Muetterties, E. L. *J. Am. Chem. Soc.* **1980**, *102*, 4541. (b) Davis, J. H.; Beno, M. A.; Williams, J. H.; Zimmie, J.; Tachikawa, M.; Muetterties, E. L. *Proc. Natl. Acad. Sci. U.S.A.* **1981**, *78*, 668.
(3) Holt, E. M.; Whitmire, K. H.; Shriver, D. F. *J. Organomet. Chem.* **1981**, *213*, 125.
(4) Bradley, J. S.; Ansell, G. B.; Leonowicz, M. E.; Hill, E. W. *J. Am. Chem. Soc.* **1981**, *103*, 4968.
(5) Bradley, J. S. *Adv. Organomet. Chem.* **1983**, *22*, 1 and references therein.
(6) Bogdan, P. L.; Woodcock, C.; Shriver, D. F. *Organometallics* **1987**, *6*, 1377.
(7) Hriljac, J. A.; Holt, E. M.; Shriver, D. F. *Inorg. Chem.* **1987**, *26*, 2943.
(8) Hriljac, J. A.; Swepston, P. N.; Shriver, D. F. *Organometallics* **1985**, *4*, 158. Kolis, J. W.; Holt, E. M.; Hriljac, J. A.; Shriver, D. F. *Organometallics* **1984**, *3*, 469.
(9) Sinfelt, J. H. *Bimetallic Catalysts: Discoveries, Concepts, and Applications*; Wiley: New York, 1983.
(10) Brookhart, M.; Green, M. L. H. *J. Organomet. Chem.* **1983**, *250*, 395.
(11) (a) Beno, M. A.; Williams, J. M.; Tachikawa, M.; Muetterties, E. L. *J. Am. Chem. Soc.* **1980**, *102*, 4542. (b) Beno, M. A.; Williams, J. M.; Tachikawa, M.; Muetterties, E. L. *J. Am. Chem. Soc.* **1981**, *103*, 1485.
(12) Wijeyesekera, S. D.; Hoffmann, R.; Wilker, C. N. *Organometallics* **1984**, *3*, 962.
(13) Harris, S.; Bradley, J. S. *Organometallics* **1984**, *3*, 1086.
(14) Shriver, D. F.; Drezdzon, M. A. *Manipulation of Air-Sensitive Compounds*, 2nd ed.; Wiley Interscience: New York, 1986.
(15) Andrews, M.; Kaesz, H. D. "MASPAN" version 4, University of California, Los Angeles, CA, 1977.

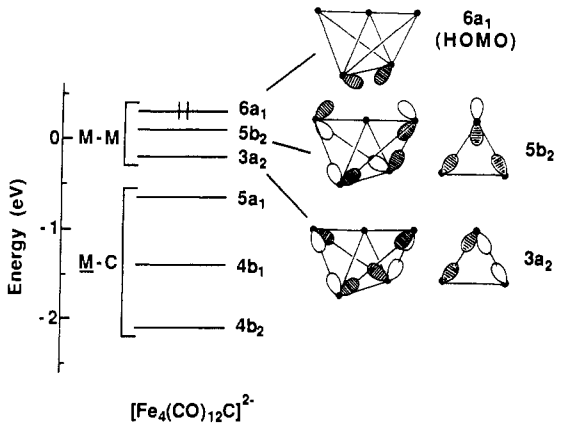

Figure 1. Calculated energies for the six highest energy occupied metal–metal- and metal–carbon-bonding orbitals in $[Fe_4(CO)_{12}C]^{2-}$. Representations of the three metal–metal-bonding orbitals are shown on the right. Two views are shown for the $5b_2$ and $3a_2$ orbitals. The views of one of the triangular "wings" of the butterfly emphasize the face-bonding character of the $5b_2$ orbital and the edge-bonding nature of the $3a_2$ orbital.

moved and the solution allowed to slowly warm to room temperature. The reaction mixture was evaporated to dryness. The oily brown solids were extracted with five or six 10-mL portions of methylcyclohexane until the extracts were colorless. The extracts were filtered, combined, and evaporated to dryness to produce a dark brown crystalline solid. This was washed with 5 mL of pentane before vacuum-drying. Yield: 0.052 g, 29%. Anal. Calcd (found) for $C_{14}H_2CrFe_3O_{13}$: C, 28.13 (28.06); H, 0.34 (0.50); Cr, 8.70 (8.34); Fe, 28.03 (27.96). Mass spectrum: parent ion at m/e 598 (MASPAN: R = 9.0% with 4% loss of 2 H) with consecutive loss of 13 CO's to $HCrFe_3(CH)^+$ (MASPAN: R = 3.0% with 12% loss of 1 H and 52% loss of 2 H).

Synthesis of $HWFe_3(CO)_{13}(CH)$. This was prepared in a manner analogous to that for the Cr analogue. Yield: 0.100 g, 49%. Anal. Calcd (found) for $C_{14}H_2WFe_3O_{13}$: C, 23.05 (23.41); H, 0.28 (0.37); W, 25.20 (24.94); Fe, 22.96 (22.42). Mass spectrum: parent ion at m/e 730 (MASPAN: R = 23.2% with 16% loss of 2 H) with consecutive loss of 13 CO's to $HWFe_3(CH)^+$ (MASPAN: R = 2.2% with 16% loss of 1 H and 50% loss of 2 H).

Calculational Details. Molecular orbital calculations were carried out for $[RhFe_3(CO)_{12}C]^-$ and $[MnFe_3(CO)_{13}C]^-$. The structure of $[RhFe_3(CO)_{12}C]^-$ has been experimentally determined.[8] Calculations were carried out for a cluster in which the atomic positions were adjusted to give an idealized C_s geometry. The structure of $[MnFe_3(CO)_{13}C]^-$ has not been determined, so calculations were based on the structure of the similar cluster $Fe_4(CO)_{13}C$.[4] A Mn atom was substituted for one of the hinge iron atoms, and atomic positions were idealized to give a cluster having C_s symmetry.

All of the results described here was obtained by Fenske–Hall molecular orbital calculations.[16] The 1s through nd functions for Mn, Fe, and Rh were taken from Richardson et al.,[17,18] while the $(n+1)$s and $(n+1)$p functions were chosen to have exponents of 2.0 for Mn and Fe and 2.2 for Rh. The carbon and oxygen functions were taken from the double-ζ functions of Clementi.[19] The valence p functions were retained as the double-ζ functions, while all other functions were reduced to single-ζ form. In all of the calculations the local coordinate system on the carbido carbon atom was oriented with the x axis parallel to a line connecting the two hinge atoms, the y axis parallel to a line connecting the two wingtip irons, and the z axis pointing out of the cluster.

Results and Discussion

Protonations. As shown by this work and an earlier study,[8] all heterometallic carbide clusters protonate at the carbide ligand to produce μ_4-η^2 bound methylidyne fragments (eq 2–5). These

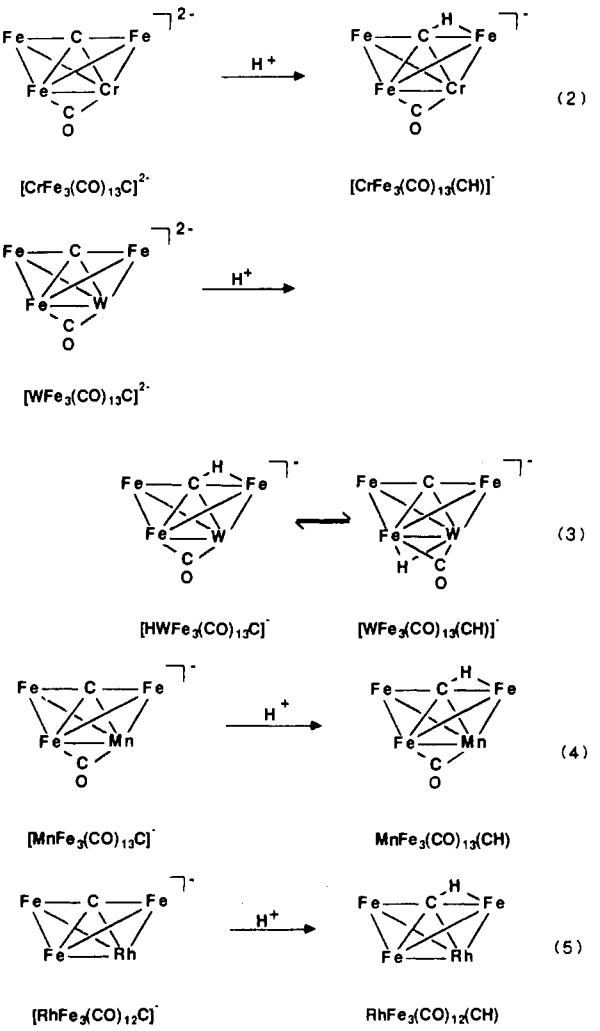

reactions were most conveniently monitored by IR spectroscopy (Table I). The formulation of the protonated products as methylidyne species is based upon the NMR data (Tables II and III). All of these compounds display a resonance in the ^1H NMR spectra in the upfield region near TMS, +2 to −2 ppm. In the ^{13}C NMR spectra the CH moiety is characterized by resonances located between 360 and 330 ppm, with $^1J_{CH}$ of approximately 105 Hz. The upfield ^1H shifts and low values for the carbon–hydrogen coupling constant are indicative of agostic interactions between the methylidyne proton atoms and the metals.[11] The NMR data are consistent with the values reported for the only other tetrametallic methylidyne cluster, $HFe_4(CO)_{12}(CH)$.[2,11] The dispositions of the CO ligands are not firmly established by the NMR and IR data, but reasonable structures are indicated for the products in eq 2–5.

In contrast with the other monoprotonated clusters, the tungsten compound exists as a mixture of methylidyne (C–H···M) and hydride (M–H–M) clusters (eq 3). The existence of the isomer containing an M–H–M moiety may be due to the greater basicity of the third-row transition-metal atom than of the first-row metals in most of the other clusters. This mixture was observed by NMR methods regardless of whether the sample was generated by low-temperature in situ protonation or dissolution of the crystalline solid at a low temperature. As reported earlier,[8] the rhodium methylidyne compound is unstable. When a solution of this species was warmed, it was observed to disproportionate (eq 6) to produce known iron[20] and iron–rhodium[7] clusters.

$$2RhFe_3(CO)_{12}(CH) \xrightarrow{\Delta} HFe_3(CO)_{10}(CH) + Rh_2Fe_3(CO)_{14}C \quad (6)$$

(16) Hall, M. B.; Fenske, R. F. *Inorg. Chem.* **1972**, *11*, 768.
(17) Richardson, J. W.; Nieupoort, W. C.; Powell, R. R.; Edgell, W. F. *J. Chem. Phys.* **1962**, *36*, 1057.
(18) Richardson, J. W.; Blackman, M. J.; Ranochak, J. E. *J. Chem. Phys.* **1973**, *58*, 3010.
(19) Clementi, E. *J. Chem. Phys.* **1964**, *40*, 1944.
(20) Kolis, J. W.; Holt, E. M.; Shriver, D. F. *J. Am. Chem. Soc.* **1983**, *105*, 7307.

Table III. ^{13}C NMR Data for Selected Cluster Carbide Derivatives[a-c]

compd	conditions	^{13}C NMR data, ppm
[PPN][$CrFe_3(CO)_{13}(CH)$]	$CD_2Cl_2/CHFCl_2$, −120 °C	349.4 (1), d, J_{CH} = 100 Hz; 241.3 (1); 237.9 (2); 221.0 (1); 216.9 (2); 215.3 (2); 214.2 (2); 211.9 (2); 211.6 (1)
[PPN][$CrFe_3(CO)_{13}(CH)$]	CD_2Cl_2, −90 °C	348.4 (1), d, J_{CH} = 100 Hz; 239.9 (1); 237.1 (2); 220.8 (1); 216.6 (2); 213.6 (6), br; 211.2 (1)
[PPN][$WFe_3(CO)_{13}(CH)$]	CD_2Cl_2, −90 °C	464.1 (1); 334.8 (2), d, J_{CH} = 107 Hz; 221.9 (1); 221.6 (2); 217.7 (4); 215.5 (4); 215.3 (1); 215.1 (2); 214.9 (4); 213.0 (12); 211.0 (1); 210.7 (1); 210.2 (2); 206.5 (2); 205.7 (1); 196.4 (1); 192.4 (1)
$RhFe_3(CO)_{12}(CH)$[d]	CD_2Cl_2, −90 °C	340, d, $^1J_{CH}$ = 102 Hz
$HCrFe_3(CO)_{13}(CH)$	CD_2Cl_2, −90 °C	357.9 (1), dd, $^1J_{CH}$ = 100 Hz, $^2J_{CH}$ = 10 Hz; 226.8 (1); 225.8 (1); 224.1 (1), d, $^2J_{CH}$ = 13 Hz; 211.6 (1); 210.9 (1); 210.4 (1); 209.1 (1); 207.8 (1); 207.2 (1); 206.6 (1); 206.2 (1); 203.8 (1); 203.6 (1)
$HWFe_3(CO)_{13}(CH)$	CD_2Cl_2, −90 °C	339.6 (1), dd, $^1J_{CW}$ = 69 Hz, $^1J_{CH}$ = 105 Hz, $^2J_{CH}$ = 10 Hz; 213.0 (1); 212.6 (1); 210.2 (1), J_{CW} = 120 Hz; 209.8 (1); 207.9 (1); 206.3 (1); 206.0 (1); 205.2 (1); 204.1 (1); 203.4 (1); 201.3 (1), J_{CW} = 148 Hz; 196.4 (1), d, J_{CW} = 119 Hz, $^2J_{CH}$ = 10 Hz; 186.2 (1), J_{CW} = 118 Hz
$MnFe_3(CO)_{13}(CH)$	CD_2Cl_2, −90 °C	335.9 (1), d, $^1J_{CH}$ = 107 Hz; 224.9 (1); 219.0 (2); 210.4 (2); 209.9 (1); 208.9 (2); 207.8 (2); 207.2 (2); 204.9 (1)
$HFe_4(CO)_{12}(CH)$[e]	toluene-d_8, −70 °C	335 (1), dd, $^1J_{CH}$ = 103 Hz, $^2J_{CH}$ = 6 Hz; 214.8 (4); 212.0 (2); 209.9 (4); 207.3 (2)

[a] All shifts in ppm downfield of TMS. [b] All resonances singlet unless noted: d = doublet; dd = doublet of doublets; br = broad. [c] The numbers in parentheses are integrated intensities. [d] Poor spectral quality precluded the assignment of the carbonyl resonances. [e] References 2a and 24.

When the anionic methylidyne clusters were treated with a second 1 equiv of acid, the proton added to the metal framework to generate a hydride cluster (eq 7). This product is similar to

$$[MFe_3(CO)_{13}(CH)]^- \xrightarrow{H^+} HMFe_3(CO)_{13}(CH) \quad (7)$$
$$M = Cr, W$$

that of the reported protonation of $HFe_4(CO)_{12}(CH)$ to produce the cationic compound $[H_2Fe_4(CO)_{12}(CH)]^+$.[21] Methylene (CH_2) species have not been observed in these reactions.

Methylation Studies. The reactivity of the four heterometallic carbide clusters with methyl trifluoromethanesulfonate was also explored. In contrast, with the two dinegative clusters $[MFe_3(CO)_{13}C]^{2-}$, M = Cr, W, the two mononegative clusters $[MnFe_3(CO)_{13}C]^-$ and $[RhFe_3(CO)_{12}C]^-$ do not react with excess methylating agent. This difference may be attributed to low nucleophilicity resulting from a single negative charge. Unfortunately, both $[CrFe_3(CO)_3C]^{2-}$ and $[WFe_3(CO)_3C]^{2-}$ yield mixtures of products. Attempts to separate the reaction products failed, but NMR spectra of the product of methylation for the chromium cluster indicate the presence of both $[Fe_3(CO)_{10}(CCH_3)]^-$ and $[Cr_2Fe_3(CO)_{16}C]^{2-}$.[7,20]

Bonding in the Heterometallic Carbides. Molecular orbital calculations were carried out for $[RhFe_3(CO)_{12}C]^-$ and $[MnFe_3(CO)_{13}C]^-$. The rhodium-containing cluster $[RhFe_3(CO)_{12}C]^-$ provides an example of a cluster in which the heterometal lies in a different period than Fe, and it is the only heterometallic butterfly carbide cluster for which an X-ray crystal structure is available. The other cluster, $[MnFe_3(CO)_{13}C]^-$, provides an example of a cluster in which the heterometal is a first-row metal. The structure of the latter cluster has not been determined, so calculations were carried out for a model cluster having the structure of $Fe_4(CO)_{13}C$ but with Mn substituted for one of the hinge Fe atoms. Although this does not give a completely accurate picture of the bonding, it does make it possible to study the effect of Mn substitution into the cluster. The calculations for these two clusters allow us to compare how two quite different heterometal atoms influence the electronic structure of the butterfly.

The results of the protonation studies described above indicate that for all the heterometallic carbide clusters the addition of one proton results in a methylidyne cluster. This behavior is different from that observed for the corresponding homometallic cluster $[Fe_4(CO)_{12}C]^{2-}$, where the addition of one proton results in a product in which hydrogen bridges the two hinge Fe atoms. It is possible that protonation on the Fe–M hinge is blocked by the hinge-bridging CO ligand for clusters containing Cr, Mn, or W. For $[RhFe_3(CO)_{12}C]^-$, however, the hinge position should be accessible to a proton, and yet protonation occurs at the carbide.

Earlier molecular orbital calculations for $[Fe_4(CO)_{12}C]^{2-}$ showed that the reactivity of the homometallic cluster toward protonation can be related to the frontier orbitals of the cluster.[13] These calculations showed that the molecular orbitals of $[Fe_4(CO)_{12}C]^{2-}$ can be divided into groups that are localized on the metal framework and groups that represent metal–carbon interactions. All of the orbitals having significant carbon character are sufficiently stabilized that the highest energy occupied orbitals contain only metal character. The energies of the six highest energy occupied orbitals are shown in Figure 1. The three highest energy orbitals are metal–metal bonding and contain no carbon character. The next three orbitals are also primarily metal based but do contain some carbon character. Representations of the three metal framework orbitals are also shown in Figure 1. It is these orbitals that correlate with the observed sites of protonation. The $6a_1$ HOMO is localized across the hinge bond, and it is this orbital that interacts with a proton to give the singly protonated cluster $[HFe_4(CO)_{12}C]^-$, in which a hydrogen atom bridges the two hinge atoms. The HOMO in $[HFe_4(CO)_{12}C]^-$ becomes the $5b_2$ orbital illustrated in Figure 1, and we have suggested previously that reaction with a second proton involves an interaction between the $5b_2$ orbital and the proton followed by a rearrangement of the cluster to allow bonding of the hydrogen atom with the carbido atom as well as a wingtip iron atom. This would result in the methylidyne-containing cluster $HFe_4(CO)_{12}(CH)$. Therefore, in the homometallic carbide cluster, the structures of the protonated clusters can be explained in terms of the calculated electronic structure.

Bonding in $[RhFe_3(CO)_{12}C]^-$. The introduction of a heterometal such as Rh or Mn brings about a number of changes in the electronic structure of the butterfly cluster.[22] The discussion here will focus on the changes in the high-energy occupied orbitals because, just as in $[Fe_4(CO)_{12}C]^{2-}$, it is these orbitals that can be related to the cluster reactivity. Two factors are responsible for the major changes in these orbitals. These are (1) the relative energies of the Fe, Rh, and Mn d orbitals and (2) the lowering of the symmetry of the cluster from C_{2v} in $[Fe_4(CO)_{12}C]^{2-}$ to C_s in $[RhFe_3(CO)_{12}C]^-$ and $[MnFe_3(CO)_{13}C]^-$.

The energies of the six highest energy occupied M–M- and M–C-bonding orbitals for $[RhFe_3(CO)_{12}C]^-$ are shown in Figure 2. Because of the C_s symmetry all of the orbitals now have a′ or a″ symmetry. The character of the high energy metal–metal-bonding orbitals in $[RhFe_3(CO)_{12}C]^-$ is considerably different from that of the corresponding orbitals in $[Fe_4(CO)_{12}C]^{2-}$. The 8a″ HOMO in $[RhFe_3(CO)_{12}C]^-$ has contributions from the iron atoms but negligible hinge rhodium character. On the other hand, the lower lying 7a″ orbital has contributions from the wingtip irons and hinge rhodium but negligible hinge iron character. These

(21) Drezdzon, M. A.; Shriver, D. F. *J. Mol. Catal.* **1983**, *21*, 81.

(22) S. Harris, manuscript in preparation.

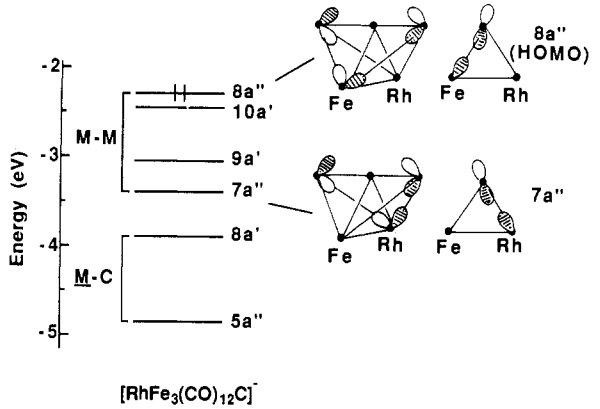

Figure 2. Calculated energies for the six highest energy occupied metal–metal- and metal–carbon-bonding orbitals in $[RhFe_3(CO)_{12}C]^-$. Representations of the metal–metal-bonding 8a″ and 7a″ orbitals are shown on the right. The views of the triangular butterfly "wings" emphasize how the hinge Fe and hinge Ru orbitals interact separately with the wingtip Fe orbitals.

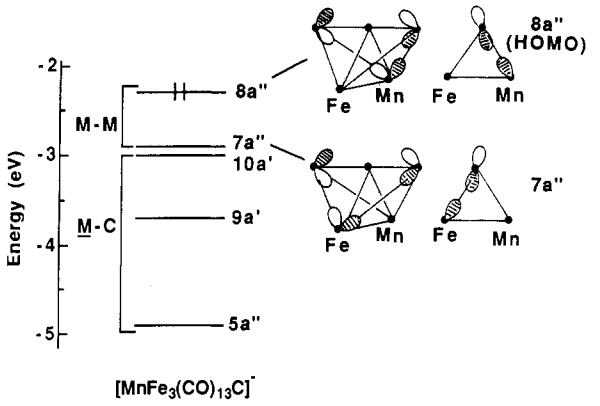

Figure 3. Calculated energies for the five highest energy occupied metal–metal- and metal–carbon-bonding orbitals in $[MnFe_3(CO)_{13}C]^-$. Representations of the 8a″ and 7a″ orbitals are shown on the right. These orbitals are very similar to the corresponding orbitals in $[RhFe_3(CO)_{12}C]^-$ except that the energies are reversed. Now the a″ orbital having heterometal character is the HOMO. This is a consequence of the relative energies of the Mn and Fe orbitals.

two a″ orbitals are illustrated in Figure 2. A comparison with the $5b_2$ and $3a_2$ orbitals of $[Fe_4(CO)_{12}C]^{2-}$ (Figure 1) shows that while in $[Fe_4(CO)_{12}C]^{2-}$ orbitals from all four metals combine to form distinct face-bonding $5b_2$ and edge-bonding $3a_2$ orbitals, in $[RhFe_3(CO)_{12}C]^-$ the wingtip Fe orbitals now form different combinations in order to interact separately with the hinge iron and rhodium orbitals. The reduced symmetry of $[RhFe_3(CO)_{12}C]^-$ allows these different combinations. Since the Rh orbitals lie lower in energy than the corresponding Fe orbitals, the combination having hinge Rh character is stabilized relative to the all-Fe combination. There is no orbital in $[RhFe_3(CO)_{12}C]^-$ that is strictly equivalent to the hinge bonding $6a_1$ orbital in $[Fe_4(CO)_{12}C]^{2-}$ because there is no orbital that is completely localized across the hinge. Instead, orbitals that in $[Fe_4(CO)_{12}C]^{2-}$ could be labeled as M–M or M–C bonding mix together so that in $[RhFe_3(CO)_{12}C]^-$ the high energy 9a′ and 10a′ orbitals are both bonding across the hinge and also both contain C p_z character. This means not only that there is no single localized hinge bonding orbital in $[RhFe_3(CO)_{12}]^-$ but also that one of the highest energy occupied orbitals now has C p_z character.

In summary, both the character and the relative energies of the frontier orbitals in $[RhFe_3(CO)_{12}C]^-$ are markedly different from those in $[Fe_4(CO)_{12}C]^{2-}$. The 8a″ HOMO in $[RhFe_3(CO)_{12}C]^-$ is an M–M-bonding orbital, but it has no Rh contribution. In the region of the two wingtip Fe atoms it most closely resembles the $5b_2$ orbital of $[Fe_4(CO)_{12}C]^{2-}$. The second and third highest occupied orbitals (9a′ and 10a′) contain both hinge metal and carbon character. The lowest energy M–M bonding orbital, 7a″, is bonding between the hinge Rh and wingtip Fe atoms and is stabilized relative to the others because of its large Rh character.

Just as for $[Fe_4(CO)_{12}C]^{2-}$, the calculated orbital structure of $[RhFe_3(CO)_{12}C]^-$ provides an explanation for the reactivity of the cluster toward protonation. The orbital analyses of $[Fe_4(CO)_{12}C]^{2-}$ and $[HFe_4(CO)_{12}C]^-$ indicated that in $[HFe_4(CO)_{12}C]^-$ the $5b_2$ HOMO is responsible for the initial attack at a wingtip Fe to ultimately yield the $HFe_4(CO)_{12}(CH)$ cluster. The calculations for $[RhFe_3(CO)_{12}C]^-$ suggest that the same type of orbital, the 8a″ HOMO, is responsible for the initial attack at a wingtip Fe to finally yield $RhFe_3(CO)_{12}(CH)$. Moreover, the second highest occupied orbital, 10a′, has C p_z character and could facilitate interaction with the carbon atom and thus formation of the methylidyne. We still might wonder why, although the initial attack by a proton comes at a wingtip, the protonated cluster does not subsequently rearrange to give a final hydride product where the hydrogen bridges the hinge Fe and Rh atoms. This type of behavior is observed for several tetrametal butterfly nitride clusters,[23] where protonation occurs via a wingtip metal but results in final product clusters in which the hydrogen bridges the two hinge metal atoms, indicating that the hydride is the energetically favored product. Although it is not possible to calculate and compare the total energies of the methylidyne and hydride products of protonation of $[RhFe_3(CO)_{12}C]^-$ (we would expect the difference in energies to be relatively small), the calculated character of the frontier orbitals of $[RhFe_3(CO)_{12}C]^-$ suggests that the absence of a very localized hinge bonding metal framework orbital may be responsible for the observed preference for the methylidyne product. The absence of the localized charge density provided by such an orbital presumably makes the hinge site less favorable for interaction with the proton, thus hampering the formation of a hinge bridging hydride and tipping the energy balance in favor of the methylidyne product.

Bonding in $[MnFe_3(CO)_{13}C]^-$. The orbital structure of $[MnFe_3(CO)_{13}C]^-$ is influenced by the bridging carbonyl ligand as well as by the C_s symmetry and the differences in energy between the Mn and Fe orbitals. The energies of the highest occupied M–M and M–C bonding orbitals for $[MnFe_3(CO)_{13}C]^-$ are shown in Figure 3. Because of the bridging CO, there are only two high-energy occupied metal–metal-bonding orbitals, 7a″ and 8a″. The hinge bonding a′ orbital interacts with the 5σ orbital of the bridging CO group to form a new low-energy a′ orbital. Previous calculations show that for $Fe_4(CO)_{13}C$ the two remaining high-energy metal-based orbitals are nearly identical with the $5b_2$ and $3a_2$ orbitals of $[Fe_4(CO)_{12}C]^{2-}$. We would expect the 7a″ and 8a″ orbitals of $[MnFe_3(CO)_{13}C]^-$ to resemble the corresponding orbitals of $[RhFe_3(CO)_{12}C]^-$. Indeed, the 7a″ and 8a″ orbitals of $[MnFe_3(CO)_{13}C]^-$ (Figure 3) are similar to the corresponding orbitals of $[RhFe_3(CO)_{12}C]^-$ in that one represents bonding between the hinge Fe and wingtip Fe atoms while the other represents bonding between the hinge Mn and wingtip Fe atoms. Now, however, because the Mn orbitals lie higher in energy than the Fe orbitals, the 8a″ HOMO contains the heteroatom contribution. The all-Fe orbital lies at lower energy. Just as in $[RhFe_3(CO)_{12}C]^-$, the 8a″ HOMO in $[MnFe_3(CO)_{13}C]^-$ resembles, in the wingtips of the cluster, the $5b_2$ orbital of $[Fe_4(CO)_{12}C]^{2-}$ and can be associated with the initial attack of a proton at a wingtip. Here it is not surprising that the final product is the methylidyne $MnFe_3(CO)_{13}(CH)$ since the hinge bridging orbital is used for bonding with the bridging CO and is thus completely unavailable.

In comparison to the case of the higher symmetry $[Fe_4(CO)_{12}C]^{2-}$, substitution of either Mn or Rh into the hinge of the cluster brings about the formation of two new metal framework orbitals that allow the hinge Fe and hinge heteroatom to interact separately with the wingtip Fe's. The relative energies of these two new orbitals are not the same in the two clusters, however,

(23) Blohm, M. L.; Fjare, D. E.; Gladfelter, W. L. *J. Am. Chem. Soc.* **1986**, *108*, 2301.

(24) Kolis, J. W. Ph.D. Dissertation, Northwestern University, 1984.

because these energies reflect the relative energies of the Mn, Fe, and Rh orbitals. In $[RhFe_3(CO)_{12}C]^-$, where the Rh orbitals are lower in energy than the corresponding Fe orbitals, the cluster orbital having heteroatom character is stabilized and the all-Fe combination is the HOMO. In $[MnFe_3(CO)_{13}C]^-$, where the Mn orbitals are higher in energy than the corresponding Fe orbitals, the cluster orbital having heteroatom character is destabilized and becomes the HOMO. Even though the HOMO's of $[MnFe_3(CO)_{13}C]^-$ and $[RhFe_3(CO)_{12}C]^-$ are different in the hinge region of the clusters, they are very similar in the wingtip region. In this region they both resemble the $5b_2$ orbital of $[Fe_4(CO)_{12}C]^{2-}$, the orbital with which we have associated protonation at the wingtip to ultimately yield a methylidyne cluster. Therefore, just as for $[HFe_4(CO)_{12}C]^-$ the character of the HOMO in both $[RhFe_3(CO)_{12}C]^-$ and $[MnFe_3(CO)_{13}C]^-$ can be associated with the site of proton attack.

Conclusion

In summary, the protonation of carbide clusters with a butterfly array of three irons and a heterometal, Cr, W, Mn, or Rh, occurs at the carbide ligand to produce an agostic C-H--Fe linkage with a wingtip iron atom. By contrast, the first site of protonation in the Fe_4 butterfly carbide cluster, $[Fe_4(CO)_{12}C]^{2-}$, is the Fe-Fe hinge. Fenske-Hall molecular orbital calculations indicate that in the Fe_4 butterfly the HOMO is largely localized on the hinge. This is consistent with protonation at this site. When either a more electronegative metal, Rh, or less electronegative metal, Mn, is introduced into a hinge position in the cluster, the metal-metal-bonding orbitals are perturbed by both the difference in energy between the iron and heterometal orbitals and the lowering of the cluster symmetry. The character and the relative energies of the resulting cluster orbitals depend on the heterometal. In $[RhFe_3(CO)_{12}C]^-$ the orbitals having Rh character are stabilized so that an all-Fe combination is the HOMO. In $[MnFe_3(CO)_{13}C]^-$, on the other hand, an orbital having Mn character is destabilized and becomes the HOMO. In $[RhFe_3(CO)_{12}C]^-$ the high-energy orbitals are further perturbed so that no single metal-metal-bonding orbital is localized across the hinge. Although the characters of the HOMO's are different in the hinge region of the two clusters, in the wingtip region the characters are nearly the same. In both cases, the HOMO extends over the wingtip atoms and correlates with the initial attack of a proton at the wingtip to ultimately form the agostic C-H-Fe bond. The final methylidyne product is not unexpected for $[MnFe_3(CO)_{13}C]^-$ because the hinge M-M bonding orbital is used for bonding with the bridging CO ligand and is thus unavailable for formation of a bridging hydride. For $[RhFe_3(CO)_{12}C]^-$, the calculations suggest that the final methylidyne product is favored over a bridging hydride because of the absence of a very localized hinge bonding orbital.

Acknowledgment. The portion of this research performed at Northwestern University was supported by the NSF Synthetic Inorganic and Organometallic Chemistry Program.

Registry No. $[PPN][CrFe_3(CO)_{13}(CH)]$, 112680-35-0; $[PPN]_2[CrFe_3(CO)_{13}C]$, 88669-42-5; $[PPN][WFe_3(CO)_{13}(CH)]$, 112680-37-2; $[PPN]_2[WFe_3(CO)_{13}C]$, 88657-60-7; $HCrFe_3(CO)_{13}(CH)$, 112680-38-3; $HWFe_3(CO)_{13}(CH)$, 88657-62-9; $[RhFe_3(CO)_{12}C]^-$, 93110-68-0; $[MnFe_3(CO)_{13}C]^-$, 93110-71-5; $[Fe_3(CO)_{10}(CCH_3)]^-$, 87698-66-6; $[Cr_2Fe_3(CO)_{16}C]^{2-}$, 109864-04-2; $[PPN][HWFe_3(CO)_{13}C]$, 112680-40-7; Cr, 7440-47-3; Fe, 7439-89-6; W, 7440-33-7; Rh, 7440-16-6; Mn, 7439-96-5.

Contribution from the Department of Chemistry, Texas A&M University, College Station, Texas 77843

Cluster Synthesis via Aggregation: Synthesis and Solution and Solid-State Characterization of Sulfur-Capped Group 6 Metal Carbonyl Clusters

Donald J. Darensbourg,* David J. Zalewski, Kathryn M. Sanchez, and Terry Delord

Received July 22, 1987

The trinuclear clusters $[PPN]_2[M_3(CO)_{12}S]$ (M = Cr, Mo, W) have been prepared by a stepwise aggregation of $[M(CO)_5]$ fragments about a sulfur atom template, with subsequent loss of three carbonyl ligands concomitant with the formation of three metal-metal bonds. The stepwise assembly process allows for the synthesis of the mixed-metal clusters $[PPN]_2[Cr_2W(CO)_{12}S]$, $[PPN]_2[Mo_2W(CO)_{12}S]$, and $[PPN]_2[CrMoW(CO)_{12}S]$. These compounds have been characterized by infrared and ^{13}C NMR spectroscopies, and X-ray crystal structures of the Cr_3, Mo_3, and Mo_2W clusters have been determined. $[PPN]_2[Cr_3(CO)_{12}S]$: space group $P2_1/c$, a = 25.732 (6) Å, b = 14.255 (5) Å, c = 21.689 (4) Å, β = 96.16 (3)°, V = 7909.8 Å^3, Z = 4. $[PPN]_2[Mo_3(CO)_{12}S]$: space group $P2_1/c$, a = 25.953 (4) Å, b = 14.329 (2) Å, c = 21.830 (5) Å, β = 96.26 (2)°, V = 8069.2 Å^3, Z = 4. $[PPN]_2[Mo_2W(CO)_{12}S]$: space group $P2_1/c$, a = 25.912 (6) Å, b = 14.275 (3) Å, c = 21.871 (3) Å, β = 96.23 (2)°, V = 8042.0 Å^3, Z = 4. The trinuclear clusters can add a fourth $[M(CO)_5]$ unit to produce the tetranuclear derivatives $[PPN]_2[M_4(CO)_{17}S]$. In solution, the carbonyl ligands of both the tri- and tetranuclear clusters are extremely fluxional. Temperatures as low as -110 °C must be achieved to freeze out the various processes.

Introduction

During the last 2 decades organometallic chemists have been actively pursuing the synthesis, chemical reactivity, and spectral/structural properties of discrete molecular transition-metal clusters.[1] Much of this interest originates from the analogy drawn between metal clusters and catalytic surfaces.[2] Polynuclear transition-metal complexes have not yet realized their anticipated potential as homogeneous catalysts;[3] however, metal clusters in and on solid supports (e.g., silica, alumina, magnesia, and zeolites) have provided highly active catalysts or catalyst precursors with surface structures often being similar to the structures of their molecular analogues.[4]

(1) (a) Johnson, B. F. B. *Transition Metal Clusters*; Wiley: New York, 1980. (b) Muetterties, E. L.; Rhodin, T. N.; Band, E.; Brucker, C. F.; Pretzer, W. R. *Chem. Rev.* **1979**, *79*, 91. (c) King, R. B. *Prog. Inorg. Chem.* **1972**, *15*, 287. (d) Canning, N. O. S.; Madix, R. J. *J. Phys. Chem.* **1984**, *88*, 2437. (e) Chini, P., *J. Organomet. Chem.* **1980**, *200*, 379 (f) Vahrenkamp, H., *Struct. Bonding (Berlin)* **1977**, *32*, 1.

(2) (a) Muetterties, E. L. *Bull Soc. Chim. Belg.* **1975**, *84*, 959. (b) Muetterties, E. L. *Bull. Soc. Chim. Belg.* **1976**, *85*, 451. (c) Muetterties, E. L. *Science (Washington, D.C.)* **1971**, *196*, 839.

(3) (a) Laine, R. M. *J. Mol. Catal.* **1982**, *14*, 137. (b) Ugo, R.; Psaro, P. *J. Mol. Catal.* **1983**, *20*, 53. (c) Muetterties, E. L.; Krause, M. J. *Angew. Chem.* **1983**, *95*, 135. (d) Ford, P. C. *Acc. Chem. Res.* **1982**, *14*, 31. (e) Marko, L.; Vizi-Orosz. In *Metal Clusters in Catalysis*; Gates, B. C., Guczi, L. Knözinger, H., Eds.; Elsevier: New York, 1986; p 89.

(4) (a) Psaro, R.; Ugo, R. In *Metal Clusters in Catalysis*; Gates, B. C., Guczi, L., Knözinger, H., Eds.; Elsevier: New York, 1986; p 427. (b) Gates, B. C. In *Heterogeneous Catalysis*; Shapiro, B. L., Ed.; Texas A&M University Press: College Station, TX, 1984; p 1. (c) Gallezot, P. In *Metal Clusters*; Moskovits, M., Ed.; Wiley-Interscience: Toronto, 1986; p 219. (d) Brenner, A. *ibid.*; p 249. (e) Gates, B. C. *ibid.*; p 283.

0020-1669/88/1327-0821$01.50/0